

# INVESTIGATION OF MESH SENSITIVITY ISSUES IN STRAIN-SOFTENING GEOMATERIALS USING FIXED MESH

<sup>1</sup>Chow Chee Meng, <sup>2</sup>Aishah Abu Bakar

<sup>1</sup>Gue & Partners Sdn Bhd, Bandar Tasik Selatan, 57000, Kuala Lumpur

<sup>2</sup>Faculty of Engineering, University of Malaya, 50603, Kuala Lumpur

e-mail: <sup>1</sup>c\_meng@tm.net.my, <sup>2</sup>aishah\_ab@um.edu.my

**Abstract.** *An investigation on mesh sensitivity issues in the computation of strain-softening geomaterials where failure is attributed to the formation and development of failure planes or shear bands are presented. Particular emphasis had been placed on geomaterials (soil) and its applicability in geotechnical engineering. However, results presented in this paper are also of relevance to any materials exhibiting strain-softening and localisation. Mesh sensitivity issues, in particular mesh ability to capture localisation and mesh size dependency, have been investigated via passive earth pressure failure problem using a cohesion-softening Mohr-Coulomb soil model and fixed mesh. Both smooth and rough retaining walls have been considered in the analyses. Results have indicated that load-displacement responses and orientations of failure plane are very much dependent on mesh size and mesh alignment when localisation is considered, especially for the non-associated case.*

## 1. Introduction

Earth structures such as retaining walls are subjected to a complex combination of loadings. The resultant force on the wall, active or passive, is dependent on the relative movement of the wall. The failure of retaining walls is often attributed to the formation and development of failure planes or shear bands. These are narrow zones of failed material, within which shear strains concentrate (i.e. localisation) and outside which unloading takes place.

Finite element computations of strain-softening and localisation is known to be highly mesh sensitive due to the fact that the classical plasticity theory is only satisfactory to describing the material response prior to the onset of localisation. Because localisation zone influences the overall behaviour of a material its size and location may within the boundary considered affect load-displacement response, resulting in a non-unique solution.

In this paper, two distinct mesh sensitivity for softening and localisation problems, mesh ability to capture localisation and element size sensitivity, are investigated by using classical plasticity theory and fixed mesh.

## 2. The cohesion-softening model

The model used in the analysis is the non-associated Mohr Coulomb soil model that has been used by Abu Bakar (1999) and based on generalised plasticity theory outlined by Nayak and Zienkiewicz (1972). The model consists of four linear components: elastic, hardening, softening and perfectly plastic. The elasto-plastic behaviour is modeled by varying the cohesion from an initial value,  $c_i$  to a peak value  $c_p$  during hardening and from a peak value,  $c_p$  to a residual value,  $c_r$  during softening; by assuming the angles of dilation and friction remain constant (Figure 1). The gradient of the hardening and softening part of the model: termed as the hardening and softening moduli respectively are defined by the incremental equation,  $h = d\bar{\sigma} / d\bar{\epsilon}^p$ ; positive for hardening and negative for softening.

The two main material parameters associated with Mohr Coulomb soil model are the angle of internal friction,  $\phi$  and cohesion,  $c$ . As the soil model is also a cohesion-softening model, other parameters relating to elastic and plastic components of the model also need to be defined. These are the Young's modulus,  $E$ , the Poisson's ratio,  $\nu$ , the angle of dilation,  $\psi$ , and the hardening and softening parameters,  $h_p$  and  $sp$ , respectively.

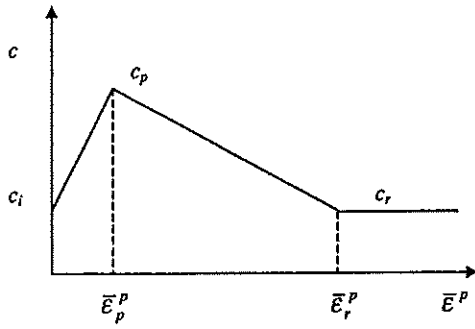


Figure 1. Variation of cohesion with plastic shear strain invariant.

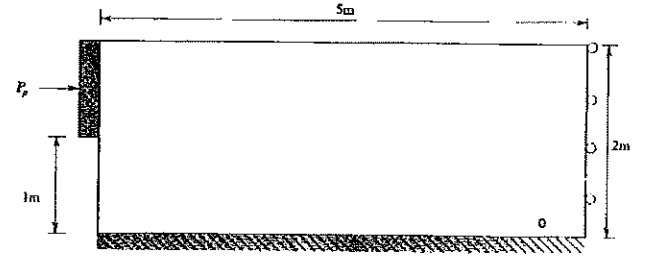


Figure 2. Geometry and boundary conditions used in the analysis of a retaining wall (after Abu Bakar (1999)).

### 3. Fixed mesh analysis

Figure 2 shows the problem geometry used in the current investigation and it is similar to that used by Abu Bakar (1999). Specifically, a rigid wall of 1m height, is pushed horizontally, and without rotation, into a drained soil mass of dimensions 2m x 5m using equal-sized displacement increments which is then solved using the elastic global stiffness matrix and the Newton-Raphson iteration scheme. The boundary conditions include a fixed base and rollers along the right had boundary allowing only vertical movement. The other two boundaries are free, allowing the nodes to move in any direction as the wall displaces. The initial stresses at each Gauss point were generated using the material unit weight,  $\gamma' = 10 \text{ kN/m}^3$ , a coefficient of earth pressure at rest,  $K_o = 1$ , and by considering the distance of the Gauss point from ground level. The analyses have been carried out for a perfectly smooth wall and a perfectly rough wall. The effect of the smooth wall has been achieved by allowing the contact nodes to move freely in the vertical direction, while for a perfectly rough wall, the effect has been achieved by restraining movement via rollers.

In the investigation, three types of mesh alignment are considered. Type A consists of elements with equal height and width, type B consists of elements with double the height (stretched vertically) and type C consists of elements with double the width (stretched horizontally). For each mesh alignment, two types of mesh density are considered: M4 and M10. For M4, there are four elements behind the wall and for M10, ten elements. Figure 3 shows example of the M4 mesh used in the analysis.

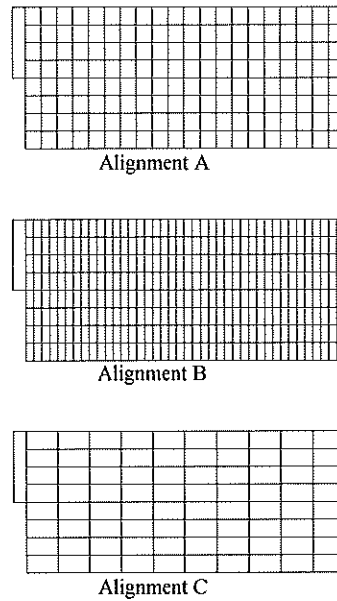


Figure 3. Meshes used for investigation of mesh alignment (M4).

In total, there are six uniform meshes of 8-node quadrilateral elements; these comprises 160 (M4) and 1000 (M10) elements for type A alignment, 320 (M4) and 2000 (M10) elements for type B alignment and 80 (M4)

and 500 (M10) elements for type C alignment, respectively. The parametric studies carried out in the work presented here for the fixed mesh analysis are summarised in Table 1. For each mesh density, the analyses have been carried out using the elastic-hardening-softening-plastic (ehsp) model. The parameter values considered are summarized in Table 2.

The resulting passive resistance,  $P_p$  acting on the wall has been back-calculated by integrating the stresses in those elements directly behind the wall; that is, all the elements connected to the wall, except for that element just below the wall base.

Table 1. Summary of parametric studies.

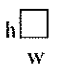
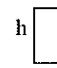
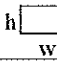
TYPE OF STUDY	DETAIL			
MESHES	mesh name		no. of elements	alignment
	A	M4	160	 $h/w = 1$
		M10	1000	
	B	M4	320	 $h/w = 2$
		M10	2000	
	C	M4	80	 $h/w = 0.5$
		M10	500	
DILATION ANGLE	type		value	
	constant		$\psi = 0^\circ$ $\psi = 30^\circ$	
SOFTENING PARAMETER	name		value (kN/m <sup>2</sup> )	
	SP1		$-1 \times 10^3$	
	SP2		$-2 \times 10^3$	
	SP3		$-3 \times 10^3$	
	SP4		$-4 \times 10^3$	

Table 2. Soil parameters used in the retaining wall analyses.

Soil parameter	Symbol	Values
Young's modulus	$E'$	$1.0 \times 10^5$ $\text{kN/m}^2$
Unit weight of soil	$\gamma'$	10.0 $\text{kN/m}^3$
Cohesion Initial	$c_i'$	1.0 $\text{kN/m}^2$
Peak	$c_p'$	5.0 $\text{kN/m}^2$
Residual	$c_r'$	1.0 $\text{kN/m}^2$
Coefficient of earth pressure at rest	$K_0$	1
Poisson's ratio	$\nu'$	0.3
Friction angle	$\phi'$	$30^\circ$
Dilation angle	$\psi$	$0^\circ, 30^\circ$
Hardening parameter	$h_p$	$3.0 \times 10^4$ $\text{kN/m}^2$
Softening parameter	$sp$	$(-1, -2, -3, -4) \times 10^3$ $\text{kN/m}^2$

### 3.1 Results and discussions

For all analyses in this investigation, the load-displacement responses of the wall are studied together with a comparison of various analytical solutions of the passive force,  $P_p$  (collapse load) and failure plane inclination,  $\theta_s$  with the numerical results obtained.

#### 3.1.1 Smooth wall

Figures 4 and 5 show the variation of passive force on the smooth wall for the associated and non-associated case respectively. From the load-displacement curve, it can be observed that the collapse and residual load is in close agreement with Rankine's limiting solutions, as expected, but much nearer the peak solution due to minimal influence of progressive failure for the smooth wall. Furthermore, it can be observed that collapse load

is hardly influenced by mesh density but the post-peak slope is noticeably steeper as the mesh density increases. This is due to the fact that, as the mesh gets finer, the shear band narrows as a function of the element size, with high strain concentration being confined within this band. The figures show that there is no tendency for the curves to converge to a unique solution. This observation has been reported by Sluys (1992), Zienkiewicz et al. (1995) and Abu Bakar (1999). Similar trends have been observed for different values of softening parameter [5].

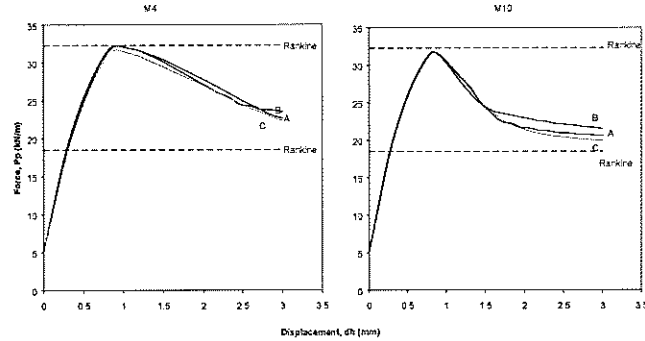


Figure 4. Load-displacement curve for smooth wall ( $\psi = 30^\circ$ , SP1)

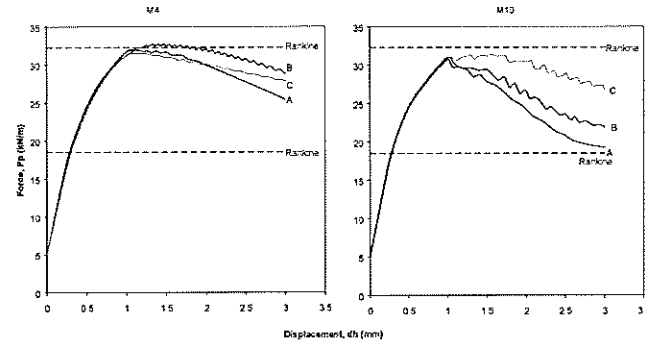


Figure 5. Load-displacement curve for smooth wall ( $\psi = 0^\circ$ , SP1)

The influence of mesh alignment on the load displacement responses is also shown in Figure 4 and 5. Results show that mesh alignment has little effect on peak load. However, the variation in the post-peak slope, especially for  $\psi = 0^\circ$ , is greater when different mesh alignment is used. For non-associated case, square alignment (alignment A) gives more stable and realistic response compared to rectangular element (alignment B and C). This could be due to the fact that formation of failure planes may be hindered in a way when rectangular elements are used. The same argument can also be used for explaining the undulating effect of the post-peak curve.

As for the effect of dilation angle,  $\psi$ , it can be observed from Figure 4 that for the non-associated case, mesh alignment B and C exhibit undulating post-peak slope. Meanwhile, for the associated case where  $\psi = 30^\circ$ , the post-peak slope is stable and did not exhibit any undulating characteristic for all types of mesh alignment, mesh density and softening parameter.

Finally, the variation of  $\theta_s$  with softening modulus for different mesh alignment is investigated. These values have been obtained from the incremental shear strain invariant contours plotted at the end of each analysis. For the non-associated case, as the mesh density and  $sp$  value increases, the failure plane orientation moves from Roscoe's to Coulomb's solution for type A mesh alignment whereas for type B and C mesh alignment, no visible trend is observed and it tends to exceed the limiting values of Roscoe and Coulomb solution. In addition, it can be observed that mesh alignment B gives the biggest value of  $\theta_s$ , alignment C the lowest and alignment A in between the two extreme values. Figure 6 shows the incremental shear strain invariant contours plotted at the end of each analysis for different mesh alignment for  $\psi = 0^\circ$ , mesh M4 and SP1. Figure 6 shows that the shear band is conveniently formed (bands of straight line) for type C alignment as compared to type B (wavy lines). This two observation confirmed results by Pastor et al. (1992) and Zienkiewicz et al. (1995) on the effect of mesh alignment; orientation of the failure plane tends to follow the alignment of the mesh.

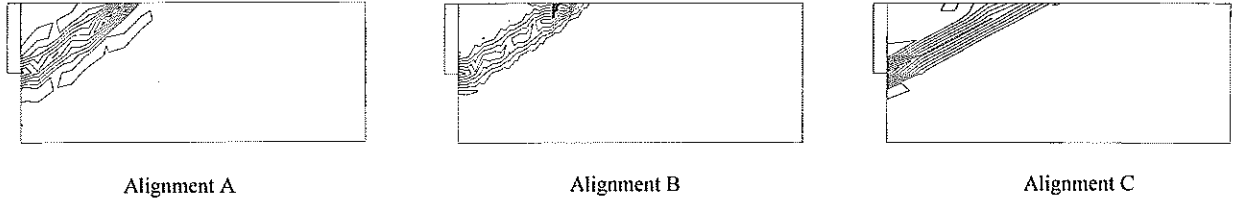


Figure 6. Contours of incremental shear strain invariant for different mesh alignment for smooth wall ( $\psi = 0^\circ$ , mesh M4, SP1)

### 3.1.2 Rough wall

For the non-associated case, the peak load is within both Sokolovski's and Caquot & Kerisel's solution (Figure 7). As for the associated case, there are instances when peak load exceeds Sokolovski's solution but nevertheless still within Caquot and Kerisel's solution (Figure 8). The figures also show that the post-peak slope is slightly less steep when wall roughness is considered. In general, the change in post-peak response is less dramatic than for the smooth wall and is even less for the non-associative flow case. For  $\psi = 30^\circ$ , mesh alignment has virtually no effect on the collapse and residual load and for  $\psi = 0^\circ$ , the effect of mesh alignment is reduced as mesh density increases.

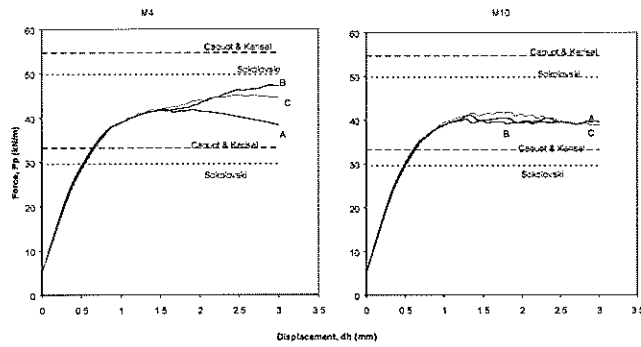


Figure 7. Load-displacement curve for rough wall ( $\psi = 0^\circ$ , SP2)

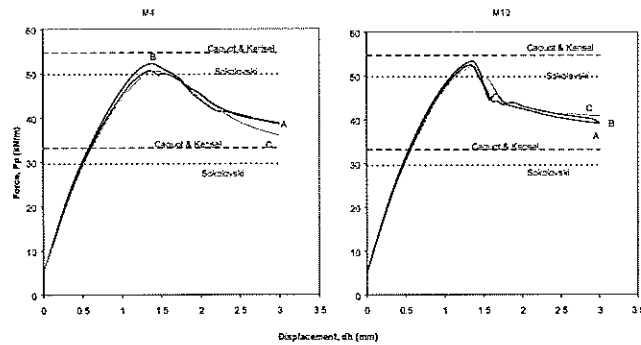


Figure 8. Load-displacement curve for rough wall ( $\psi = 30^\circ$ , SP2)

The influence of wall roughness is significant when considering the shape and orientation of the critical failure surface. Figure 9 shows the rupture surfaces obtained from the computer simulation for  $\psi = 30^\circ$ , mesh M10 and SP1 using the strain-softening model. It can be seen that mesh alignment A generate the best failure surface with both the primary rupture surface (log spiral curve followed by a straight line) and the secondary rupture surface (straight line emerging from the top of the wall and progressing obliquely downward) clearly visible whereas for alignment B and C, the rupture surface is not clear, especially for alignment C where the log spiral part and the secondary rupture surface failed to materialise. In addition, Figure 10 shows that as the mesh density increases, the secondary rupture surface becomes more distinct.

Finally, for the rough wall,  $\theta_s$  is measured as the angle made by the straight portion of the primary rupture surface to the horizontal and is referred to as the breakout angle. For the non-associative flow rule,  $\theta_s$  tends to move from Roscoe's solution to Arthur's solution as the mesh gets finer and the  $sp$  value gets higher for type A

mesh alignment. For mesh alignment B and C, it is similar to smooth wall and displays no visible trend as the mesh density and  $sp$  value increases and tends to exceed the limiting value of Roscoe's and Coulomb's solution.

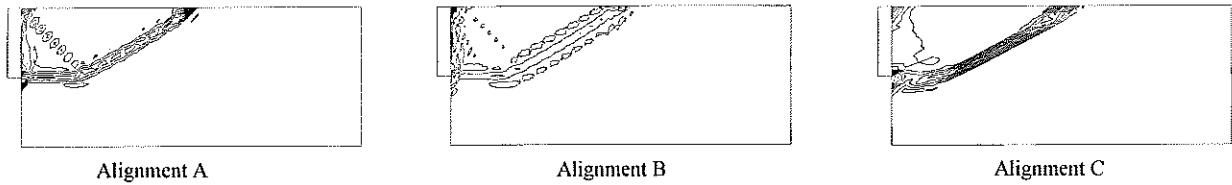


Figure 9. Contours of incremental shear strain invariant for different mesh alignment for rough wall ( $\psi = 30^\circ$ , mesh M10, SP1)

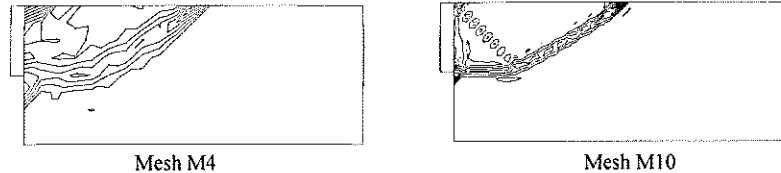


Figure 10. Contours of incremental shear strain invariant for mesh density M4 and M10 for rough wall ( $\psi = 30^\circ$ , mesh alignment A, SP1)

#### 4. Conclusion

The issues of mesh sensitivity in strain-softening computation have been investigated for passive earth pressure failure using classical plasticity theory and fixed mesh finite element approaches. A wide range of results has been presented for smooth and rough retaining walls and comparisons made with various analytical solutions. The investigation has produced a number of important findings summarised below:

a) *Load-displacement response*

The load displacement response after the peak load suffers from mesh dependency, i.e. mesh alignment and mesh density affects the gradient of the post-peak slope. The effect becomes significant when non-associated flow rule ( $\psi = 0^\circ$ ) is considered.

b) *Orientation of failure surface*

Failure plane orientation is influenced by mesh alignment, with the orientation tends to follow the mesh alignment.

c) *General failure mechanism*

From the analysis using fixed mesh, the failure surface for smooth wall is correctly formed, i.e. a single straight failure surface extending from the base of the wall to the soil surface. However, for rough wall, mesh alignment does affect the proper formation of failure surface especially in log-spiral part and the secondary failure surface.

d) *Analytical comparisons*

Computed failure plane orientations,  $\theta_s$ , vary according to mesh alignment and angle of dilation used. For non-associated case for smooth wall,  $\theta_s$  moves from Roscoe's to Coulomb's solution with increasing strain-softening and mesh density, for type A (square) alignment only. As for non-associated case for rough wall,  $\theta_s$  moves from Roscoe's to Arthur's solution with increasing strain-softening and mesh density, again for type A (square) alignment only.

In conclusion, computations of localisation involving strain-softening require greater care and attention as solutions derived from such computations are highly sensitive to mesh density, mesh alignment and even angle of dilation.

## 5. References

- [1] Abu Bakar, A., "Adaptive and Fixed Mesh Investigation of Localisation in Strain-softening Geomaterials", Ph.D. Thesis, University of Manchester, Manchester, 1999.
- [2] Arthur, J. R. F., Dunstan, T., Al-Ani, G. A. A. L. and Assadi, A., "Plastic deformation and failure in granular media", *Geotechnique* 27, No. 1, 1977, pp. 53-74.
- [3] Arthur, J. R. F. and Dunstan, T., "Rupture layers in granular material", *Proc. IUTAM Symp. Deformation and Failure of Granular Materials*. Delft (Eds. P. A. Vermeer & H. J. Luger), Rotterdam, Balkema, 1982, pp. 453-459.
- [4] Caquot, A. and Kerisel, J., "Tables for Calculation of Passive Pressure, Active Pressure and Bearing Capacity of Foundations", Gauthier-Villars, Paris, 1948.
- [5] Chow, C.M., "Investigation of Mesh Sensitivity Issues in Strain-Softening Geomaterials using Fixed Mesh", B.Eng. Thesis, University of Malaya, Kuala Lumpur, Malaysia, 2001.
- [6] Craig, R. F., "Soil Mechanics", 6th Edition, London, England, E & FN Spon, 1998.
- [7] Nayak, G.C. and Zienkiewicz, "Elasto-plastic stress analysis, a generalization for various constitutive relations including strain softening", *Int. J. Num. Meths. Engng*, 5, pp. 113-135, 1972.
- [8] Pastor, M., Rubio, C., Mira, P., Peraire, J., Vilotte, J. P. and Zienkiewicz, O. C., "Numerical analysis of localization", *Numerical Methods in Geomechanics*. (Eds. Pande & Pietruszczak), Balkema, Rotterdam, 1992, pp. 339-348.
- [9] Roscoe, K. H., "Tenth Rankine Lecture: The influence of strains in soil mechanics", *Geotechnique* 20, No. 2, 1970, pp. 129-170.
- [10] Sluys, L. J., "Wave Propagation, Localisation and Dispersion in Softening Solids", Dissertation, Delft University of Technology, 1992.
- [11] Smith, I. M. and Griffiths, D. V., "Programming the Finite Element Method", 2nd Edition, Chichester, England, John Wiley & Sons, 1988.
- [12] Sokolovski, V. V., "Statics of Soil Media", London, Great Britain, Butterworth Scientific Publications, 1960.
- [13] Zienkiewicz, O. C. and Taylor, R. L., "The Finite Element Method", 4th Edition (Volume 2), London, UK, McGraw-Hill, 1991.
- [14] Zienkiewicz, O. C., Huang, M. and Pastor, M., "Localization problems in plasticity using finite elements with adaptive remeshing", *International Journal for Numerical and Analytical Methods in Geomechanics*, Vol. 19, 1995, pp. 127-148.